Assignment of the ^1H and ^{15}N NMR Spectra of *Rhodobacter capsulatus* Ferrocytochrome c_2[†]

Paul R. Gooley,[‡] Michael S. Caffrey,[§] Michael A. Cusanovich,[§] and Neil E. MacKenzie*[,‡,§]

Department of Pharmaceutical Sciences and Department of Biochemistry, University of Arizona, Tucson, Arizona 85721

Received August 23, 1989; Revised Manuscript Received October 25, 1989

ABSTRACT: The peptide resonances of the ^1H and ^{15}N nuclear magnetic resonance spectra of ferrocytochrome c_2 from *Rhodobacter capsulatus* are sequentially assigned by a combination of 2D ^1H-^1H and ^1H-^{15}N spectroscopy, the latter performed on ^{15}N-enriched protein. Short-range nuclear Overhauser effect (NOE) data show α-helices from residues 3-17, 55-65, 69-88, and 103-115. Within the latter two α-helices, there are three single 3_{10} turns, 70-72, 76-78, and 107-109. In addition αH-NH_{i+1} and αH-NH_{i+2} NOEs indicate that the N-terminal helix (3-17) is distorted. Compared to horse or tuna cytochrome *c* and cytochrome c_2 of *Rhodospirillium rubrum*, there is a 6-residue insertion at residues 23-29 in *R. capsulatus* cytochrome c_2. The NOE data show that this insertion forms a loop, probably an Ω loop. ^1H-^{15}N heteronuclear multiple quantum correlation experiments are used to follow NH exchange over a period of 40 h. As the 2D spectra are acquired in short time periods (30 min), rates for intermediate exchanging protons can be measured. Comparison of the NH exchange data for the N-terminal helix of cytochrome c_2 of *R. capsulatus* with the highly homologous horse heart cytochrome *c* [Wand, A. J., Roder, H., & Englander, S. W. (1986) *Biochemistry 25*, 1107-1114] shows that this helix is less stable in cytochrome c_2.

The cytochrome c_2 of photoheterotrophic bacteria is functionally unique as it acts as an electron carrier common in both the photosynthetic and respiratory pathways (Baccarini-Melandri et al., 1978). The high-resolution X-ray crystal structure of the cytochrome c_2 from *Rhodospirillium rubrum* (Salemme et al., 1973; Bhatia, 1981) has been solved, and preliminary analyses of the crystal quality of cytochrome c_2 from *Rhodobacter capsulatus* (Holden et al., 1987) and *Rhodobacter viridis* (Miki et al., 1986) have been published. A detailed comparison of the cytochrome c_2 of *R. rubrum* and horse heart cytochrome *c* shows that the two proteins are structurally homologous (Salemme et al., 1973). It is well established that the cytochromes c_2 and mitochondrial cytochrome *c* have a cluster of lysines surrounding the exposed heme edge and that these lysines play an important role in controlling electron transfer with a variety of physiological and nonphysiological electron donors (Tollin et al., 1986; Cusanovich et al., 1988). Furthermore, it appears that for cytochrome c_2 the same site is involved in the interaction with both the ubiquinol-cytochrome c_2 oxidoreductase (bc_1 complex)[1] and reaction center; thus, cytochrome c_2 must undergo a rotation during electron transport.

The cytochromes c_2 exhibit various physiological and biochemical differences including a variety of isoelectric points and oxidation-reduction potentials (Meyer & Kamen, 1982). Kinetic studies of the effect of ionic strength on the interaction of horse heart cytochrome *c* or *R. rubrum* or *R. capsulatus* cytochrome c_2 with the reaction center of *R. rubrum* showed that the rate-limiting process is independent of ionic strength at high cytochrome concentrations for horse heart and *R. rubrum* but dependent for *R. capsulatus* (Rickle & Cusanovich, 1979). There also appear to be differences in the functional necessity of cytochrome c_2. Deletion of the cytochrome c_2 gene from *R. capsulatus* did not prevent the bacteria from growing, photosynthetically or by respiration (Daldal et al., 1986). Gene deletion studies for *Rhodobacter sphaeroides* show that the presence of cytochrome c_2 is required for photosynthetic but not respiratory growth of this bacterium.

The recent cloning of the *R. capsulatus* gene and the availability of plasmids which can be introduced into photoheterotrophic bacteria have permitted various mutants of the *R. capsulatus* cytochrome c_2 to be produced (Caffrey et al., unpublished results). These mutants can be used, for example, to address the importance of the individual lysines that are involved in the interaction with the bc_1 complex and reaction center and also the importance of several highly conserved residues in maintaining the redox potential. To address these questions, it is essential to understand in detail the effect of each point mutation on the tertiary structure of the protein. Modern NMR techniques that are presently available allow proteins of up to 20 kilodaltons to be studied in detail (Wand et al., 1989; Redfield & Dobson, 1988; Torchia et al., 1988). Although the determination of the 3D structure of proteins of this size is a formidable task, high-quality 3D structures are being produced, for smaller proteins, that can distinguish subtle structural changes between wild-type and single-point mutations (Folkers et al., 1989). NMR has already proved to be a valuable technique in the study of basic biochemical questions of the cytochromes, for example, the conformation of the axial heme ligands (Senn & Wüthrich, 1983), the folding and dynamics (Wand et al., 1986), and the structural and dynamic effects of site-directed mutagenesis (Pielak et

[†] This work was supported by the Arizona Research Laboratories Division of Biotechnology and by Grants BRSGS07-RR07002 and RR05605 from the National Institutes of Health (to N.E.M.).

* Address correspondence to this author at the Department of Pharmaceutical Sciences, College of Pharmacy, University of Arizona.

[‡] Department of Pharmaceutical Sciences.

[§] Department of Biochemistry.

[1] Abbreviations: bc_1 complex, ubiquinol-cytochrome c_2 oxidoreductase; NMR, nuclear magnetic resonance; 2D, two dimensional; DQF-COSY, 2D double quantum filtered correlated spectroscopy; TOCSY, 2D total correlated spectroscopy; R-COSY, 2D relayed COSY; DR-COSY, 2D double-relayed COSY; NOE, nuclear Overhauser enhancement; NOESY, 2D NOE-correlated spectroscopy; HMQC, 2D ^1H-detected heteronuclear multiple quantum spectroscopy; Y75F, Tyr→Phe-75 *R. capsulatus* cytochrome c_2; P35A, Pro→Ala-35 *R. capsulatus* cytochrome c_2.

0006-2960/90/0429-2278$02.50/0

al., 1988a,b). The detailed ^1H assignments of horse heart cytochrome *c* have been published (Wand et al., 1989), and some ^1H and directly observed ^{15}N studies have assigned a number of resonances of the *R. rubrum* cytochrome c_2 [see Senn and Wüthrich (1983) and Yu and Smith (1988), respectively].

The initial step of a detailed NMR study requires the tedious task of near-complete assignment of the NMR spectra of the protein. The sequential assignment technique has been extensively used to assign ^1H spectra of proteins (Wüthrich, 1986). Englander and Wand (1987) recently proposed a technique, the main chain directed (MCD) analysis, that utilizes the repeating pattern of secondary structure elements to aid sequential assignment without prior extensive assignment of side chain protons. Despite experimental refinements in these techniques, an extensive study requires repeated experiments at various temperatures and pH conditions to resolve resonance overlap problems encountered, particularly in the ^1H spectra of proteins of greater than 10 kilodaltons. This problem of overlap is further exacerbated for proteins with a high helical content as this element of secondary structure reduces the chemical shift dispersion of the NH protons.

A benefit of cloning and overproducing proteins is that the protein can usually be efficiently enriched with ^{13}C and ^{15}N isotopes. Recent publications have shown that the complete assignment of ^{13}C and ^{15}N spectra is possible by following the complete coupling network of individual amino acids and of sequential residues (Stockman et al., 1989). A number of ^1H-detected heteronuclear experiments have been proposed that may further aid ^1H and heteronuclear assignment. The ^1H–^{15}N HMQC–NOESY and HMQC–TOCSY experiments can resolve some overlap problems encountered in the usual analysis of the ^1H 2D spectra (Gronenborn et al., 1989).

This paper shows that the combination of ^1H–^1H NOESY, TOCSY, and DQF-COSY and ^1H–^{15}N HMQC–NOESY and HMQC–TOCSY allows near-complete assignment of the ^1H and ^{15}N backbone resonances of *R. capsulatus* ferrocytochrome c_2 at one set of sample conditions. Furthermore, the utility of ^{15}N enrichment of the protein and ^1H–^{15}N HMQC spectroscopy allow the calculation of rate constants for NH protons that exchange within several hours.

Materials and Methods

Protein Purification and Sample Preparation. The cytochrome c_2 gene was introduced into a *R. capsulatus* cytochrome c_2 minus strain (Daldal et al., 1986), details of which are to be published elsewhere (Caffrey et al., unpublished results). The recombinant bacteria were grown by respiration (aerobic, dark) on RCVB minimal media (Weaver et al., 1975) supplemented with tetracycline (2.5 μg/mL) in a 16-L fermentor. ^{15}N-enriched cytochrome c_2 was obtained by replacing the nitrogen source in the media with $(^{15}NH_4)_2SO_4$ (Isotech, Inc.). Cytochrome c_2 was purified essentially according to the method of Bartsch (1978) except that cell extracts were prepared by sonication (3 × 1 min bursts) and cell debris was removed by centrifugation at 130000*g* for 2 h.

Samples of ferrocytochrome c_2 were prepared by reducing the protein with dithionite, dialyzing, and concentrating to 2–3 mM in 45 mM phosphate/0.5 mM dithiothreitol, pH 6 at 4 °C. Samples were flushed with argon prior to capping the NMR tube. For experiments in H_2O, samples were prepared with 10% D_2O.

NMR Spectroscopy. All NMR spectra were acquired on a Bruker AM-500 equipped with an ASPECT 3000 computer. Additional hardware on this instrument included the SE-451 receiver, a "reverse" broad-band probe, and a 5-W BFX-5 X-nucleus decoupler. Temperature was controlled by a combination of a Haake thermostat and a Bruker variable-temperature controller. All two-dimensional spectra were recorded in pure absorption with time-proportional phase incrementation (TPPI) (Redfield & Kuntz, 1975). The solvent resonance was suppressed by selective irradiation during the preparation period of 1 s.

Two-dimensional ^1H–^1H spectra were usually acquired with a spectral width of 10000 Hz, 800–900 t_1 points, 2K or 4K data points in t_2, and 64, 80, or 96 transients for each t_1 point. Conventional pulse sequences were used for DQF-COSY (Rance et al., 1983), R-COSY, and DR-COSY (Wagner, 1985), TOCSY (Braunschweiler & Ernst, 1983; Davis & Bax, 1985), and NOESY (Jeener et al., 1979). The TOCSY sequence included z-filters (Rance, 1987) before and after the spin lock period. Only the decoupler channel with an additional 2-dB attenuator was used for this experiment. Pulses for both the preparation and spin lock periods were as short as possible, 15–20 μs, without causing undue sample heating. A delay, 2.4 times the 90° pulse, was inserted between each pulse of each block of the MLEV-17 spin lock period (Ernst, 1988). This delay, experimentally determined, minimized ROE effects particularly in experiments with long spin lock periods. For both the NOESY and TOCSY experiments, the coherence of the phase of the signal and of the receiver was optimized to minimize base-line distortion (Bax & Marion, 1988). NOESY spectra were recorded in H_2O and D_2O with a mixing time of 100 ms. An R-COSY was recorded in H_2O with a delay of 30 ms, and a DR-COSY was similarly recorded with an initial delay of 25 ms and a second delay of 30 ms.

Two-dimensional ^1H–^{15}N spectra were acquired with spectral widths of 10000 Hz for ^1H and 5000 Hz for ^{15}N, 4K data points in t_2, and 96 transients for each of 500 t_1 points. The pulse sequences for HMQC–NOESY and HMQC–TOCSY were according to Gronenborn et al. (1989) except that an MLEV16 spin lock was used in the HMQC–TOCSY and ^{15}N decoupling was employed only during acquisition in both experiments.

NH exchange was followed by using a series of ^1H–^{15}N HMQC spectra (Bax et al., 1983). The spectral width for ^1H was 3600 Hz and for ^{15}N was 2500 Hz. A total of 100 t_1 points of 2K data points were acquired. Eight transients preceded by four dummy scans were averaged for each t_1 point, giving a total time of 30 min per experiment. The 3 mM protein sample was prepared as described above at 4 °C, except that the buffer was prepared with 99.9% D_2O. This buffer was introduced to the sample 80 min prior to the sample being placed in the spectrometer. Spectra were acquired at 30 °C with the time midpoints being 50, 80, 110, 155, 265, 430, 685, 1035, 1545, and 2460 min after been placed in the spectrometer. Exchange was followed by measuring peak volumes assuming an elliptical shape and a radius of 10 data points. Volume measurements in "empty" regions of the spectra were used to estimate background errors. As the sample was not removed from the spectrometer, no significant change to the peak volumes of the slowly exchanging protons, that were chosen as internal references, was observed. Rate constants were calculated by exponential least-squares analysis of plots of $I = Ae^{-kt}$, where I = (peak volume) − (average background error).

All 2D spectra were processed on a VAX 8600 using FTNMR (Hare Research). Prior to 2D Fourier transformation, the data were multiplied by shifted sine bells in both t_1 and t_2 and zero-filled to yield a matrix 2048 × 2048 of real data points, except for the NH exchange experiments where

a matrix 1024 × 1024 of real data points was produced. To reduce t_1 noise, the first row was halved before Fourier transformation in the t_1 dimension (Otting et al., 1986). The degree of shift of the sine bell and the number of data points covered depended on the experiment and whether resolution or sensitivity enhancement was desired.

Results

Assignment of the ^1H and ^{15}N Spectra: Sequential Connections. Our assignment strategy followed essentially a sequential approach. As described below, the TOCSY spectra are of such a high quality that identification of spin systems was relatively easy. In part, however, the principle idea of the main chain directed (MCD) technique is used by searching for NOE patterns characteristic of helix irrespective of the extent of assignment of individual spin systems. As previously commented by Wand et al. (1989), the MCD analysis is not ideally suited to the cytochromes, as for this family of proteins up to 50% helix and no sheet is expected. Nevertheless, a sensible approach to the assignment of any protein is to locate the regular repeating units of structure by tracing the equally repeating NH–NH_{i+1} or αH–NH_{i+1} NOE patterns, together with any other NOEs that eliminate ambiguities and progressively "remove" these assigned segments from the spectrum. After the regular segments are assigned, the more difficult nonrepeating parts of the protein can be assigned in a much simplified spectrum. The initial stage of the assignment involves recognition of at least part or full spin systems. This task is difficult by COSY alone and thus, in addition, requires an experiment that describes indirect couplings. The problem is compounded for the cytochromes due to the presence of the heme prosthetic group. Despite an obvious advantage that the heme increases the dispersion of resonances, many spin systems display unusual chemical shifts up to 4–5 ppm from their expected positions, for example, the resonances of His-17 and Met-96 (Senn & Wüthrich, 1983; Wand et al., 1989).

DQF-COSY spectra resolved at least 80% of the NH–αH connectivities. This experiment was important as αH resonances were located at −0.65, 1.95, 2.38, and 2.80 ppm which in TOCSY and R-COSY experiments could easily be confused with side chain protons. The Gly spin systems were difficult to observe in this experiment, presumably from cancellation of the cross-peak due to its antiphase character and the size of the NH–αH coupling. Alternatively, TOCSY spectra with mixing times of 40–70 ms showed the complete spin system for most residues including Gly (Figure 1). This experiment has the advantage that the cross-peaks are in-phase compared to COSY spectra where individual cross-peak components are 180° out-of-phase with respect to each other, thus tending to cancel the cross-peak (Davis & Bax, 1985). The disadvantage of the TOCSY experiment is that indirect couplings cannot be simply assigned for residues containing γH, δH, or ϵH protons, the so-called long-chain residues. At this stage, however, the aim is to simply classify spin systems into residue type and not the assignment of proton type. The observed NH–αH–βH (NH–αH_2 for Gly) couplings for 103 residues, 6 NH–αH, and 2 NH–βH accounted for the 111 residues that contain the NH–αH moiety. As the αH protons for the latter two residues resonate at less than 0.02 ppm from the water resonance, their NH–αH connectivities are obscured by solvent suppression. These connectivities are observed in similar experiments at 40 °C. In the TOCSY spectrum, a number of spin systems could be completely assigned to residue type without additional information (Figure 1). These included 4 of 8 Val, 12 of 15 Ala, 4 of 7 Thr, and 10 of 13 Gly. In addition, the NH–αH–βH_2 of 15 of the 29 AMX spin systems was recognized and the observation of indirect couplings to γH protons, typical of the 8 Glu, defined 5 spin systems to belong to this residue type and indirect couplings to ϵH protons, typical of the 17 Lys, defined 10 of these spin systems. Thus, over half of the NH–αH–βH systems could be readily assigned to residue type or class of residue.

The next stage involves connecting sequential peptide units by short-range ($i, <i + 5$) NOEs. A summary of the short-range NOEs for *R. capsulatus* cytochrome c_2 is described in Figure 2. As the cytochromes contain approximately 50% helix, NOEs characteristic of this element of secondary structure are initially assigned. These NOEs are the NH–NH_{i+1}, NH–NH_{i+2}, αH–NH_{i+2}, and αH–NH_{i+3} connectivities (Wüthrich, 1986; Wagner et al., 1986). NOEs that are observed between the side chain protons and NH_{i+1} support the assignments. The procedure was extremely successful for connecting the residues of the C-terminal helix Gly-103 to Lys-115 and the central helices Asp-55 to Phe-65, and Glu-69 to Asp-88 (Figure 3). Problems of overlapping resonances made the complete assignment of the N-terminal helix difficult, and a number of ambiguities were present for the remainder of the protein. However, the combination of ^1H–^{15}N HMQC–NOESY and ^1H–^1H NOESY permitted this helix and the other parts of the protein to be sequentially connected.

There are several advantages offered by ^1H–^{15}N HMQC–NOESY. First, the absence of a diagonal allows sequential connectivities to be observed that otherwise are difficult or impossible to resolve in ^1H–^1H spectroscopy. Second, NH resonances that overlap with aromatic resonances give rise to ambiguities in interpreting the NOE data, thus, the absence of the aromatic resonances gives a valuable simplification of the spectrum. Third, where NH resonances have the same ^1H chemical shift, they are likely to be resolved in the ^{15}N dimension. Finally, establishing the connectivities already defined in the ^1H–^1H NOESY substantiates assignments without resorting to changing sample conditions such as temperature or pH. It is found, however, that in the ^1H–^{15}N HMQC–NOESY there are potentially a number of ambiguous assignments due to overlapping ^{15}N chemical shifts and that only the combination of this experiment and the ^1H–^1H NOESY could near complete sequential assignment be attained.

A part of a ^1H–^{15}N HMQC–TOCSY is shown in Figure 4. In this spectrum, all peptide NH resonances, the N(1)H of Trp-67, the $N_\epsilon H$ His-17, and the γNH_2 of Asn-11 and -36, show correlations. All these correlations are clearly resolved except that Phe-10 overlaps Lys-86 and Thr-74 overlaps one γNH of Asn-11. Thus, the ^1H–^{15}N HMQC spectrum is potentially an excellent means for following and observing spectral changes in experiments that investigate dynamics of the protein as described below for a preliminary study of NH exchange of this cytochrome c_2. The NOE connectivities for the N-terminal helix are described in the combined ^1H–^1H NOESY and ^1H–^{15}N HMQC–NOESY spectra of Figure 5. The connectivities between Thr-15 and His-17 show that resonances that would otherwise be near each other on the diagonal (Figure 5B) are readily resolved (Figure 5A). Furthermore, in the ^1H spectrum, the NH resonances of Cys-16 and His-17 overlap with the ring protons of Tyr-48, introducing an ambiguity that is resolved in the ^1H–^{15}N experiments. In Figure 4, the ^{15}N resonances of Phe-10, Asn-11, and Lys-12 are almost coincident. As the NH resonances are sufficiently resolved in the ^1H dimension, NH–NH_{i+1} connectivities are clearly established in Figure 5B.

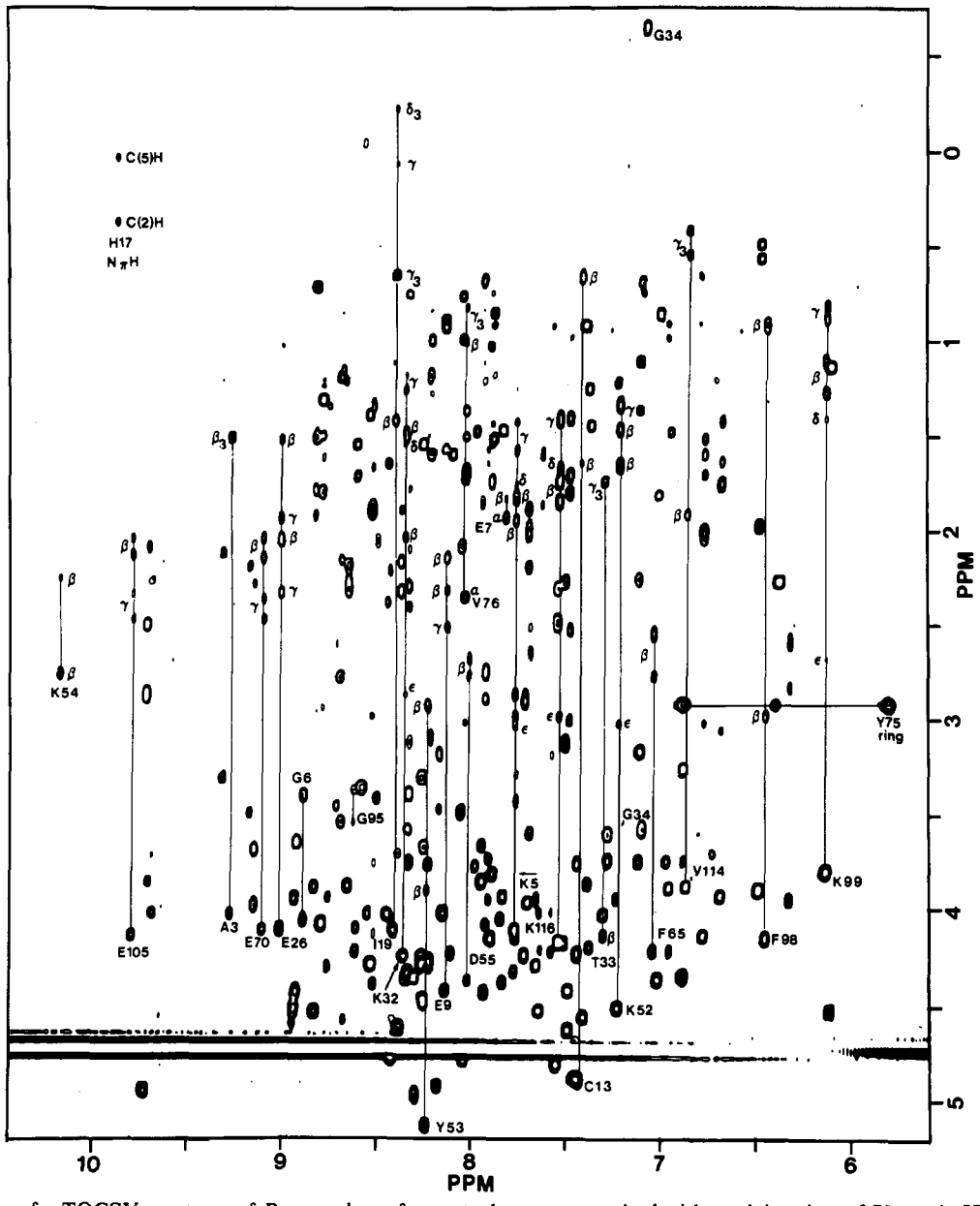

FIGURE 1: Section of a TOCSY spectrum of *R. capsulatus* ferrocytochrome c_2 acquired with a mixing time of 70 ms, in H_2O at 30 °C and pH 6. Complete spin systems are described for a number of residues including several Lys, Glu, Thr, Gly, and AMX residues. The highly shifted αH protons of Glu-7 and Val-76 are indicated. In addition, connectivities from the $N_\pi H$ to the C(2)H and C(5)H of His-17 and from the ring protons of Tyr-75 (Figure 8) to a resonance at 2.92 ppm are shown.

The NH resonances of Leu-37 and Tyr-38 are coincident with the resonances of Lys-84 and Glu-85, respectively (Table I). These two dipeptide units are connected by NH–NH_{i+1} NOEs, and thus the connectivities almost perfectly overlap in the ^1H–^1H NOESY spectrum (Figure 5B). In the ^1H–^{15}N HMQC–NOESY of Figure 5A, the NH moieties of these residues have different ^{15}N chemical shifts; therefore, the NH–NH_{i+1} connectivities are clearly resolved in this spectrum. Similarly, NH–NH_{i+1} NOEs connect Gly-80 to Ala-81 and Ala-109 to Tyr-110. The NH resonances of Gly-80 and Ala-81 precisely overlap with Tyr-110 and Ala-109, respectively; therefore, in Figure 5B, only one cross-peak is observed for these two connectivities. In Figure 5A, as these NH groups have different ^{15}N chemical shifts, the NH–NH_{i+1} NOEs are clearly established. The unambiguous assignment of these units is then substantiated by connectivities with neighboring residues and by comparing the chemical shifts of the spin systems determined in ^1H–^1H TOCSY and ^1H–^{15}N HMQC-TOCSY experiments.

At this point, connectivities could be established, in spectra acquired at 30 °C and pH 6, for almost the entire protein. All Pro except Pro-35 were connected by αH–δH_{i+1} NOEs in NOESY experiments in D_2O. Connectivities between Pro-22 and Asp-23, Gly-34 and Pro-35, Lys-54, and Asp-55, Pro-79 and Gly-80, Lys-93 and Ser-94, and Gly-95 and Met-96 could not be established at pH 6 and 30 °C. The αH's of Lys-54 and -93 resonate near the water resonance, and thus αH–NH_{i+1} connectivities from the succeeding residues will be obscured. In a NOESY spectrum acquired at 40 °C, these connectivities are observed. The αH of Pro-79 and one of the αH protons of Gly-80 resonate near each other; thus, αH–NH_{i+1} NOEs may not be resolved for this connectivity. The reasons for the absence of the remaining missing sequential connectivities are not known.

Assignment of Side Chain Protons. The next task, after the sequential assignment of the backbone protons of the protein, is the assignment of the remaining side chain protons to both a specific residue and a specific proton type. Most

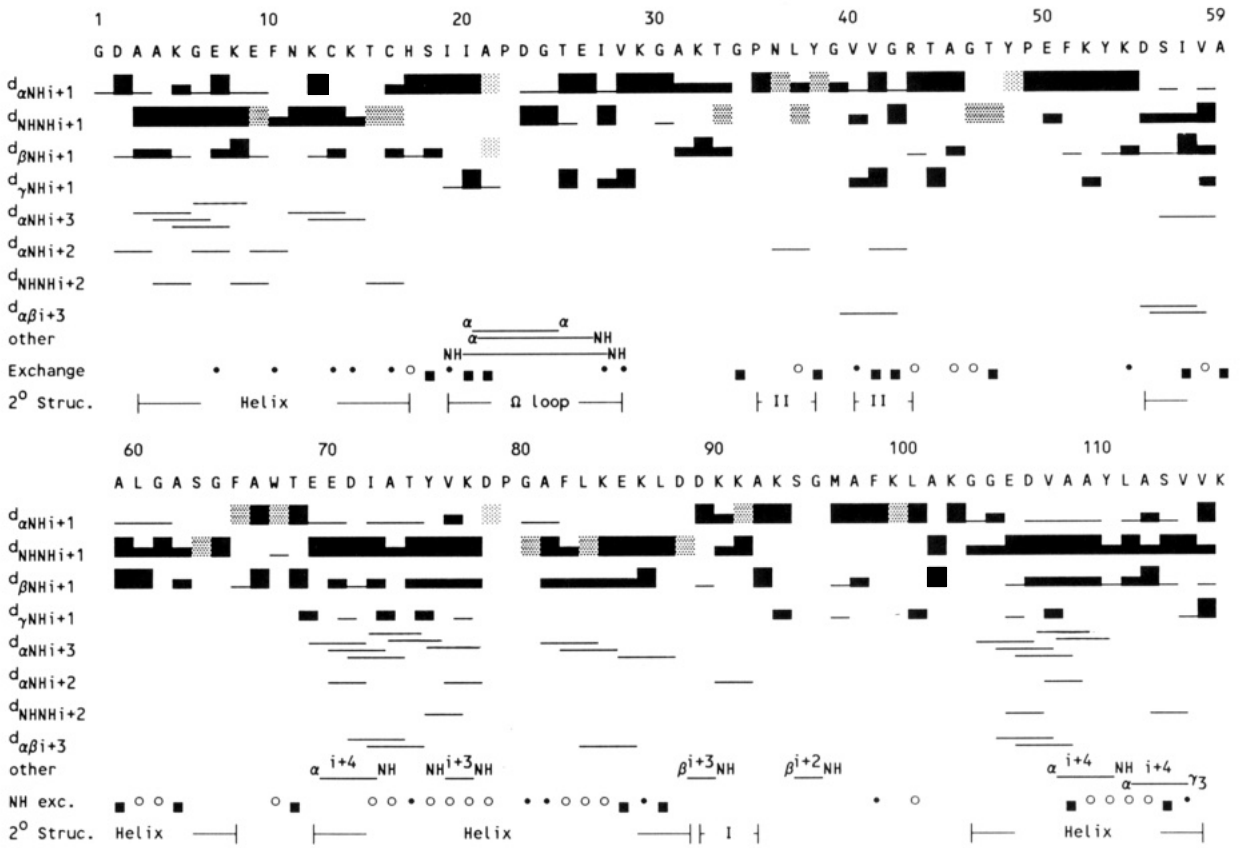

FIGURE 2: Summary of the short-range NOEs (i to $<i + 5$) observed in ^1H–^1H NOESY and ^1H–^{15}N HMQC–NOESY spectra of *R. capsulatus* ferrocytochrome c_2. Spectra were acquired with a mixing time of 100 ms in H_2O at 30 °C and pH 6. $d_{\alpha NHi+1}$ NOEs for Lys-54 to Asp-55 and for Lys-93 to Ser-94 are observed at 40 °C. Black bars indicate NOEs observed in ^1H–^1H NOESY or ^1H–^{15}N HMQC–NOESY spectra, dark stippled bars indicate NOEs ambiguous in ^1H–^1H NOESY are resolved in ^1H–^{15}N HMQC–NOESY spectra. Light stippled bars indicate $d_{\alpha\delta i+1}$ or $d_{\beta\delta i+1}$ NOEs from Pro residues. Several long-range NOEs (i to $>i + 5$) are indicated for the segment 19–28 which appears to span a Ω loop. Qualitative intensities are described by the thickness of the bar. The type of secondary structure as suggested by the NOE data is described. Protons that show slow and intermediate NH exchange rate constants (k_m, min^{-1}) are categorized as follows: <0.0001 (○); 0.0001–0.001 (■); and >0.001 (●).

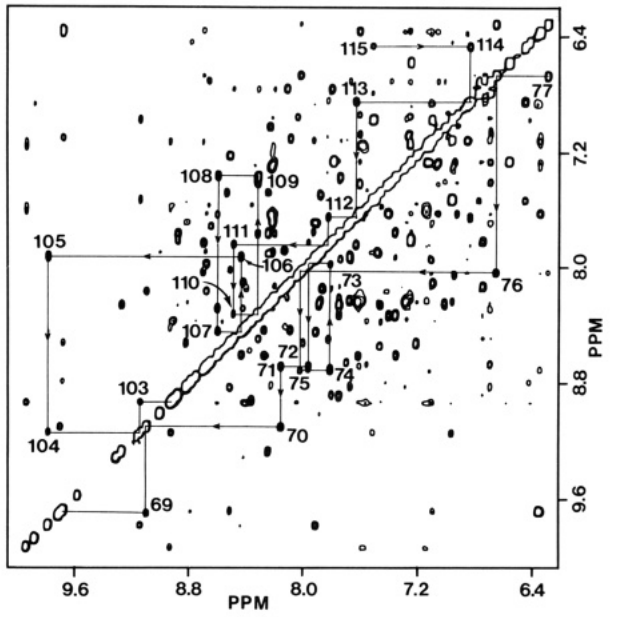

FIGURE 3: Section of a NOESY spectrum of *R. capsulatus* ferrocytochrome c_2. The spectrum was acquired with a mixing time of 100 ms in H_2O at 30 °C and pH 6. $d_{NHNHi+1}$ connectivities are described for a part of the long central helix Glu-69 to Asp-78 in the lower half of the spectrum and the C-terminal helix Gly-103 to Lys-116 in the upper half. The i to $i + 1$ connectivities are labeled for the ith proton.

of these protons could be assigned by a combination of DQF-, R-, and DR-COSY, TOCSY, and NOESY spectroscopy. The ^1H and ^{15}N assignments for *R. capsulatus* cytochrome c_2 are described in Table I. From a single TOCSY spectrum, acquired in H_2O with a mixing time of 70 ms, the complete spin systems for 65 of 74 Ala, Thr, Val, Gly, and the NH–αH–βH_2 portion of the AMX residues were assigned by following connectivities from the NH proton (Figure 1). The NH–αH–βH_2 fragments of Tyr-48 and -75 were assigned from correlations in NOESY spectra acquired in H_2O and TOCSY and DQF–COSY experiments in D_2O. A βH of Tyr-110 is coincident with a βH of Ser-94, and as the αH's of these residues are coincident, connectivities from the NH resonances are ambiguous. This ambiguity is clarified by βH–βH′ connectivities for both spin systems in TOCSY spectra. The NH–γH_3 of Thr-74 and the NH–βH_3 correlations of Ala-112 are not well resolved in TOCSY experiments. These connectivities can be clarified by following correlations from the αH protons of both residues. The αH proton of Val-76 resonates at 2.38 ppm (Figure 1). We observe connectivities from this proton and its coupled NH to resonances at 1.03 and 0.84 ppm in TOCSY spectra, but no connectivities are observed in DQF-COSY and R-COSY experiments from either the αH or the NH. In addition, a resonance at 1.71 ppm shows TOCSY and DQF-COSY cross-peaks to the resonances at 1.03 and 0.84 ppm, but not to the αH or NH. The resonance at 1.71 ppm must belong to Val-76 as similar but significantly shifted connectivities are observed for this spin system in a mutant of cytochrome c_2, Y75F (unpublished data). For the remaining residues, Val-107 and Ser-113, only one γH_3 and one βH resonance, respectively, are observed. Degeneracy is

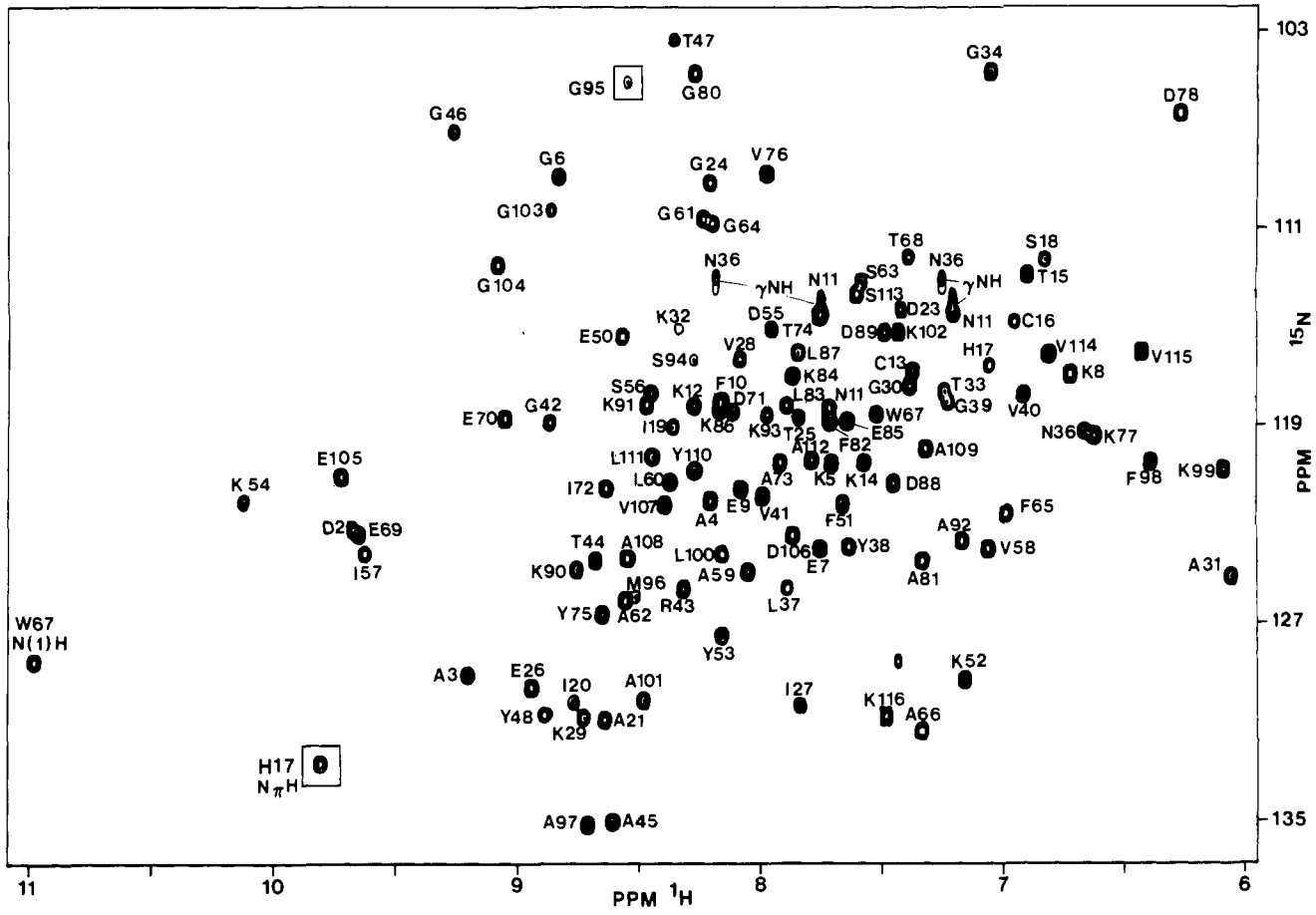

FIGURE 4: Section of a ^1H–^{15}N HMQC–TOCSY of *R. capsulatus* ferrocytochrome c_2. The spectrum was acquired with a mixing time of 70 ms in H_2O at 30 °C and pH 6. The protein was approximately 90% enriched with ^{15}N. Each peptide ^{15}N resonance that is expected to be correlated with a proton is observed and assigned. In addition, correlations for the γNH of Asn-11 and -36, the N(1)H of Trp-67, and the $N_\pi H$ of His-17 are observed in this experiment. The ^{15}N chemical shifts of the $N_\pi H$ of His-17 and peptide NH of Gly-95 are outside of this plot region (Table I). These correlations are shown boxed in the figure.

a possibility, although cross-peak shape does not agree with this suggestion.

There are 38 long-chain residues: 1 Arg, 1 Met, 5 Ile, 6 Leu, 8 Glu, and 17 Lys. The protons of the side chains of these systems are difficult to unambiguously assign based simply on the expected chemical shift. This caution is especially true for proteins that contain groups such as aromatic rings and heme moieties that can shift a proton several ppm from its expected position. As the efficiency of magnetization transfer in the TOCSY experiment is not simply a factor of position in the spin system, we cannot rely on relative peak intensity with respect to mixing time as a clear indicator of proton type. Nevertheless, the quality of the 70-ms TOCSY experiment is sufficient to at least assign resonances to a specific spin system (Figure 1). Correlations are observed to the final proton in many long-chain spin systems, for example, εH for 10 of 17 Lys and the γH for 6 of 8 Glu. For the 5 Ile, 6 Leu, single Met and Arg, connectivities from the NH to almost all other protons, in each spin system, are observed for only Ile-20 (Figure 1). This clear difference between the ionizable and hydrophobic residues must be a consequence of the former being predominantly surface residues, thus having additional motion, and the latter being buried and thus more restricted in motion.

To obtain unambiguous assignment of proton type, R-COSY and DR-COSY spectra of cytochrome c_2 were acquired in H_2O at 40 °C. It is noted that in identical experiments at 30 °C there were problems in observing adequate cross-peak intensities, presumably due to short T_2 times. In a R-COSY spectrum with a delay of 30 ms, connectivities from the NH resonance to a single βH resonance for 29 of the 38 long-chain spin systems are observed, and to both βH resonances for another 3, assigned to Lys. For the remaining six residues, Glu-7 and -69, Lys-14, -32, and -84, and Ile-57, no relay connectivities were observed. As only very weak NH–βH correlations are observed in TOCSY spectra at 30 or 40 °C, for most of these residues it was not surprising that no indirect connectivities are observed. Weak correlations for these spin systems may be from inefficient transfer of magnetization and short T_2 times. For Lys-32, however, a complete spin system is observed in TOCSY spectra acquired at 30 °C (Figure 1). At 40 °C, no correlations are observed from the NH resonance in NOESY, TOCSY, or R-COSY experiments. The analogous Lys in *R. rubrum* cytochrome c_2 is a surface residue, and therefore the most likely reason for the absence of these correlations of Lys-32 in *R. capsulatus* cytochrome c_2 is transfer of saturation from the solvent resonance. In a DR-COSY, with a first delay of 25 ms and a second delay of 30 ms, connectivities are observed to the second βH for 14 of an expected 33 long-chain residues. A number of these connectivities are shown in Figure 6. The cross-peak shape for the NH to βH correlation in TOCSY or DR-COSY experiments (Figure 6) indicates that the βH protons are probably degenerate for another six of these spin systems. Excluding the residues where a connectivity to neither βH could be established, there remain seven residues where connectivities to a second βH are not observed: Arg-43, Leu-60, -83, -87, and -111, Met-96, and Glu-105. All Leu spin systems, except

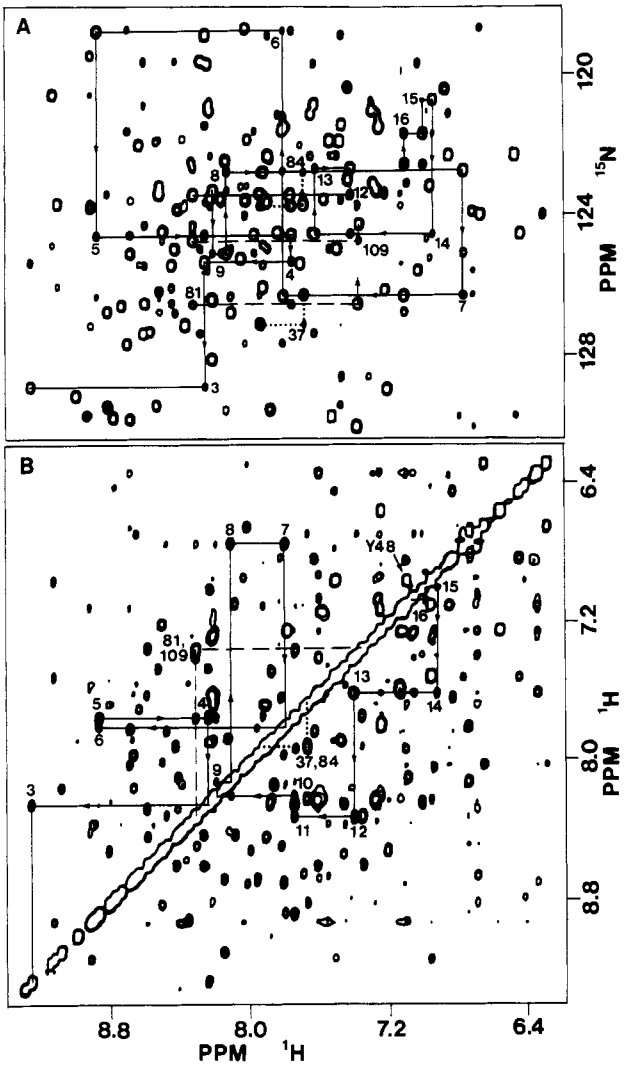

FIGURE 5: Sections of (A) ^1H–^{15}N HMQC–NOESY and (B) ^1H–^1H NOESY spectra of *R. capsulatus* ferrocytochrome c_2. The spectra were acquired with mixing times of 100 ms in H_2O at 30 °C and pH 6. The protein used in (A) was approximately 90% enriched in ^{15}N. $d_{NHNHi+1}$ connectivities for the N-terminal helix Ala-3 to His-17 are described in both spectra. The i to $i + 1$ connectivities are labeled for the ith proton. Note that in (A) the connectivities for the segment Thr-15 to His-17 are clear and unambiguous whereas in (B) the cross-peaks for the same segment are near the diagonal and the NH resonances of Cys-16 and His-17 overlap with the ring protons of Tyr-48. In (B), overlapping resonances prevent connecting, unambiguously (···) Leu-37 to Tyr-38 and Lys-84 to Glu-85 or (– –) Gly-80 to Ala-81 and Ala-109 to Tyr-110. In (A), ^{15}N chemical shift differences for these residues clarify the connectivities. Similarly, in (A), the ^{15}N chemical shifts for Phe-10, Asn-11, and Lys-12 overlap. However, the spin systems of these residues are easily connected in (B).

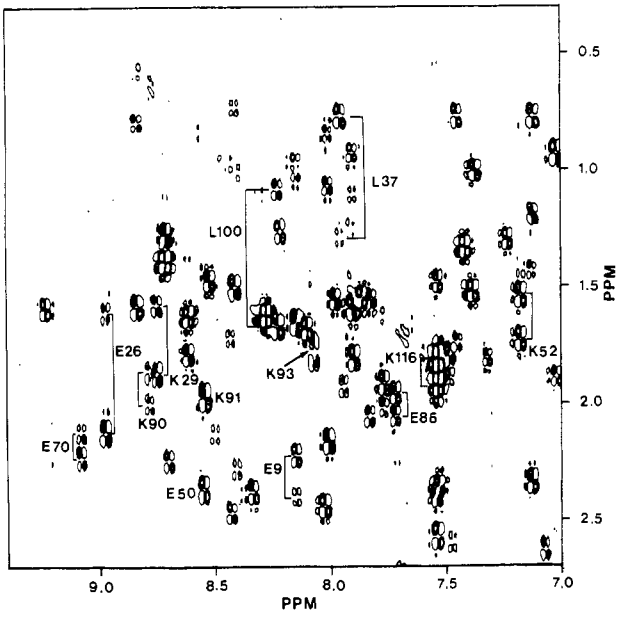

FIGURE 6: Part of a DR-COSY spectrum of *R. capsulatus* ferrocytochrome c_2. The spectrum was acquired with a first delay of 25 ms and a second delay of 30 ms in H_2O at 40 °C and pH 6. Several correlations from the NH to both βH protons for several long-chain residues (Lys, Glu, and Leu) are shown. In addition, cross-peaks that are believed to belong to degenerate βH protons are indicated for several residues.

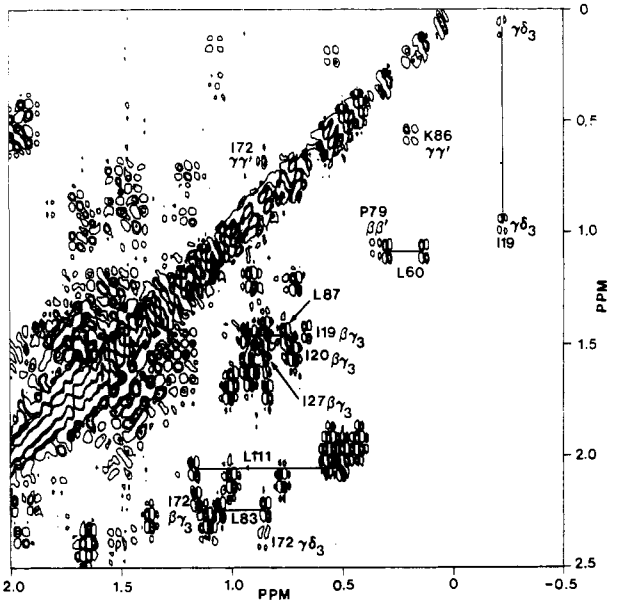

FIGURE 7: Section of a DQF-COSY spectrum of *R. capsulatus* ferrocytochrome c_2. The spectrum was acquired in D_2O at 30 °C and pH 6. Connectivities for the γH–$(\delta H_3)_2$ fragment of several Leu are described. These connectivities could not be observed for Leu-100 in this spectrum, but weak cross-peaks are observed in TOCSY spectra that can be connected to the assigned NH–αH–βH_2 fragment for this residue. The resonances for Leu-37 are outside this part of the spectrum. Additional cross-peaks assigned to four of the five Ile, the shifted βH of Pro-79, and γH of Lys-86 are indicated.

Leu-100, are easily assigned by establishing γH–δH_3 connectivities in DQF-COSY spectra (Figure 7) and linking these fragments to the respective assigned NH–αH–βH_2 fragments. Possible degeneracy of resonances prevents the complete assignment of Leu-100 (Table I). The resonances of Met-96 are well resolved due to ring current effects of the heme, and thus the assignment of this side chain is easily achieved. The assignment of the second βH resonance of Arg-43 and Glu-105 depended on intensity differences of the individual resonances in each spin system in TOCSY spectra, and thus these assignments are tentative. The assignment of Ile residues has proved particularly difficult. The shifted resonances of Ile-19 and -72 are completely assigned, but for the other three Ile overlapping resonances prevent complete and unambiguous assignments (Figure 7, Table I). Assignment of the γH of Glu spin systems is easily achieved for all except the highly shifted resonances of Glu-7. Correlations are observed from the NH to ϵH for 10 of 17 Lys in TOCSY spectra at 30 °C, and another two correlations for Lys-90 and -102 are resolved at 40 °C. In general, the ϵH resonances of individual Lys show connectivities with δH resonances in DQF-COSY, and the remaining γH protons were assigned from correlations of NH to γH and for γH to ϵH in TOCSY spectra.

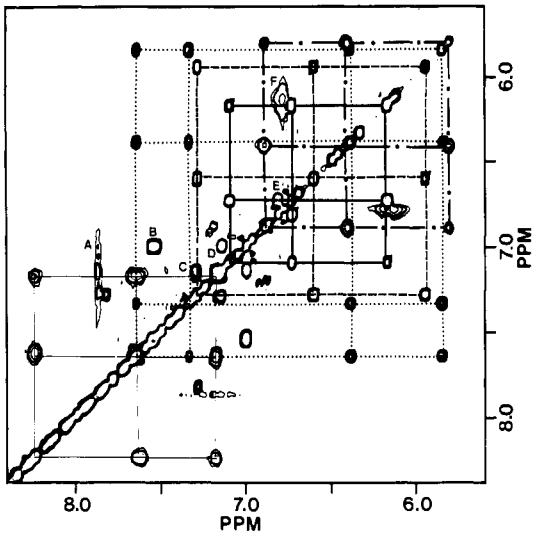

FIGURE 8: Aromatic region of the same TOCSY spectrum described in Figure 1. Connectivities are indicated for (···) Trp-67, (—) Tyr-53, (- - -) Phe-10, (thick lines) Phe-65, and (●—●) Tyr-75. Single cross-peaks are indicated for (A) Phe-51, (B) Phe-98, (C) Phe-82, (D) Tyr-48, (E) Tyr-38, and (F) Tyr-110. An additional connectivity between these protons for Tyr-75 and a resonance at 2.92 ppm is shown in Figure 1.

Identification of Pro spin systems is made by analysis of TOCSY and DQF-COSY spectra. Initial assignments of the αH and δH protons are from NOE connectivities to neighboring spin systems (Figure 2). These assignments were supported after correlating each NH–αH–βH fragment, thus eliminating all αH–βH connectivities in the crowded αH–βH region except the αH–βH, δH–δH′, and several γH–δH correlations of the Pro residues. In addition to these correlations, two apparent systems remain at 4.63–3.72 ppm and at 3.66–2.95/3.16 ppm. These systems may be the propionates of the heme, although the AMX character of the latter system does not agree with this conclusion. Similarly, no NOEs have been observed to these systems, suggesting that a contaminant may be present.

In DQF-COSY and TOCSY experiments at 30 °C and pH 6, correlations for the five Phe, five Tyr, and single His and Trp residues are observed. Characteristic of the cytochromes, the C(2)H and C(5)H resonances of His-17 are shifted by approximately 6 ppm upfield from expected positions (Figure 1) (Senn & Wüthrich, 1983; Wand et al., 1989). The N_πH proton is slowly exchanging, suggesting that it is hydrogen bonded, probably to the carbonyl of Pro-35, analogous to *R. rubrum* cytochrome c_2 (Salemme et al., 1973). TOCSY cross-peaks are observed from this proton to both C(2)H and C(5)H (Figure 1), but as expected, an NOE is observed only to C(2)H. NOEs from both βH protons to C(5)H connect the ring to its sequentially assigned NH–αH–βH_2 fragment. A part of a TOCSY spectrum describing the connectivities of the other ring spin systems is shown in Figure 8. The ring protons of Trp-67 show characteristic connectivities for this spin system and are easily connected by intraresidue NOEs to the assigned NH–αH–βH_2 segment. In TOCSY and DQF-COSY spectra, the ring protons of Tyr-38 and -48 and Phe-10 and -65 give rise to patterns typical for these residues (Wüthrich, 1986). The ring protons of Phe-82 and -98 each give a single cross-peak in DQF-COSY. In TOCSY spectra, the cross-peaks are distorted, suggesting that the H(4) proton resonates near the H(2,6) protons for Phe-82 and near the H(3,5) protons for Phe-98 (Figure 8). Of the remaining four aromatic residues, Tyr-53, -75, and -110 and Phe-51, only Tyr-53 shows cross-peaks in DQF-COSY. In TOCSY spectra, however, the ring protons of these four residues show either complex coupling patterns (Tyr-53 and -75) or broad connectivities (Phe-51 and Tyr-110), indicating that these rings flip at slow and intermediate rates, respectively, on the NMR time scale (Figure 8). In addition, a resonance at 2.92 ppm is correlated with the other protons of Tyr-75 (Figure 1). As this ring is located near the heme, strong ring current shift effects are expected. Intense intraresidue NOEs from the H(2,6) protons to the NH–αH–βH_2 fragments of Tyr-38 and Phe-10, -65, -82, and -98 are observed, thus specifically assigning these ring spin systems. Broad, but clear intraresidue NOEs are observed from the H(2,6) resonances to the assigned NH–αH–βH_2 fragment of Tyr-110. Two weak NOEs and one very weak NOE from the βH protons to ring protons are observed for Tyr-75 and -53, respectively, but no intraresidue NOEs are observed between the very broad ring protons of Phe-51 and its NH–αH–βH_2 protons. In NOESY spectra at 40 °C, where the ring resonances of Phe-51 are not as broad, intraresidue NOEs are still not observed. In addition to this problem, intense NOEs are observed from the H(2,6) protons of Tyr-48 to the αH–βH_2 protons of Phe-51. An exchangeable proton that shows NOEs to the H(3,5) protons of Tyr-53, assigned to its OH proton, also shows an NOE to the NH of Tyr-48 and at 40 °C weak NOEs to both βH protons of this residue. Furthermore, the NH of Tyr-48 shows weak NOEs to the ring protons of Tyr-53. While these important NOEs indicate that these protons of Tyr-48 and -53 and Phe-51 are in close proximity to each other, they may confuse the assignments, in particular, suggesting that the ring assigned to Phe-51 may be Tyr-48 and vice versa. The assignments, however, are confirmed in a comparison to the spectra of a cytochrome c_2 mutant, P35A, where the ring of Phe-51 shows a cross-peak pattern typical of a Phe residue (Gooley et al., unpublished results).

Secondary Structure. The summary of short-range NOEs in Figure 2 permits a qualitative assessment of secondary structure. Helices extend between residues 3–17, 55–65, 69–88, and 103–115. The intense αH–NH_{i+1} NOEs in the N-terminal helix suggest that this helix is distorted. Characteristic i to $i + 1$ and i to $i + 2$ NOEs for reverse turns are indicated for residues 35–38 (type II), 40–43 (type II), and 89–92 (type I). Interestingly, a number of long-range NOEs (i, $i + 6$ to $i + 9$) are observed between residues 19 and 28, suggesting a Ω loop is present in this region (Leszczynski & Rose, 1986). The remainder of the protein appears to be nonregular, but ordered structure.

NH Exchange. In a ^1H–^{15}N HMQC experiment, all resonances not coupled to ^{15}N are filtered from the spectrum, thus leaving the region upfield of water clean of resonances. The ^1H spectral width for this experiment can therefore be reduced to cover the NH resonances without the consequence of foldover. Furthermore, as the peptide ^{15}N resonances cover a narrow frequency range, approximately 2500 Hz at 50.7 MHz, this spectral width can be narrowed to select only these resonances. Therefore, a ^1H–^{15}N HMQC experiment can be acquired in a very short period of time, in our case less than half an hour with realistic t_2 (285 ms) and t_1 (40 ms) times and obtaining excellent resolution in both dimensions. With the use of minimal phase cycling ($90°_{\pm x}$ on the first nitrogen pulse) and two dummy scans, acquisition times may be reduced to less than 10 min, but at the expense of reduced signal to noise and the introduction of artifacts. This experiment is potentially useful in following phenomena such as intermediate NH exchange that previously could only be studied by one-dimensional techniques on well-resolved NH resonances.

Table I: ^1H and ^{15}N Chemical Shifts of *R. capsulatus* Cytochrome c_2[a]

residues	chemical shifts (ppm)					residues	chemical shifts (ppm)				
	^{15}N	NH	αH	βH	others		^{15}N	NH	αH	βH	others
Gly-1			3.78, 3.56			Ser-56	117.97	8.55	4.41	4.12, 3.75	
Asp-2	123.48	9.73	4.97	2.88, 2.50		Ile-57	124.45	9.69	4.04	1.64[b]	
Ala-3	129.38	9.27	4.04	1.54		Val-58	124.30	7.12	3.76	2.28	γH$_3$ 1.13, 1.38
Ala-4	122.30	8.26	4.31	1.57		Ala-59	125.20	8.12	4.25	1.62	
Lys-5	120.79	7.76	4.13	1.83, 1.96	γH 1.45, 1.61; δH 1.75; εH 3.05	Leu-60	121.60	8.44	4.05	2.22, 1.20	γH 1.06; δH$_3$ 0.12, 0.29
Gly-6	109.21	8.89	4.08, 3.42			Gly-61	110.94	8.30	4.98, 4.35		
Glu-7	124.27	7.81	1.95	1.85[b]		Ala-62	126.41	8.62	4.24	1.57	
Lys-8	117.21	6.78	4.15	(2.02)[c]	γH 1.53, 1.61; δH 1.73; εH 3.04	Ser-63	113.45	7.64	4.55	4.01,[g] 4.21	
						Gly-64	111.12	8.25	4.47, 3.68		
Glu-9	121.87	8.14	4.44	2.15, 2.32	γH 2.51	Phe-65	122.89	7.04	4.24	2.79, 2.57	H(2,6) 6.69, H(3,5) 7.07, H(4) 6.14
Phe-10	118.29	8.21	4.33	3.09, 3.14	H(2,6) 7.26, H(3,5) 6.57, H(4) 5.93						
Asn-11	118.57	7.78	4.34	2.86, 2.99	γNH$_2$ 7.80, 7.26; γ^{15}N 114.42	Ala-66	131.66	7.40	4.58	0.94	
						Trp-67	118.81	7.58	4.25	3.18, 4.03	H(2) 7.47, H(4) 7.62, H(5) 6.36, H(6) 5.82
Lys-12	118.53	8.33	4.36	2.30, 2.41	γH 2.12, 1.81; δH (2.13)[c]; εH 3.30, 3.24						H(7) 7.31, N(1)H 11.03, ^{15}N(1) 128.82
Cys-13	117.09	7.43	4.90	0.67, 1.67							
Lys-14	120.81	7.66	4.74	1.62, 1.88[b]							
Thr-15	113.20	6.95	3.90	4.23	γH$_3$ 1.47	Thr-68	112.47	7.45	4.90	4.66	γH$_3$ 1.40
Cys-16	115.13	7.01	4.38	0.86, 1.80		Glu-69	123.63	9.71	3.88	2.30[b]	γH 2.08[b]
His-17	116.88	7.12	3.19	1.13, 0.69	H2 0.41, H5 0.06, N$_\pi$H 9.88, ^{15}Nπ 168.61	Glu-70	118.99	9.12	4.13	2.15, 2.07	γH 2.40, 2.47
						Asp-71	118.73	8.17	4.93	3.81, 3.48	
						Ile-72	121.85	8.69	3.56	2.17	γH 0.88, 0.65; γH$_3$ 1.16; δH$_3$ 2.38[h]
Ser-18	112.61	6.88	4.37	3.28, 3.74							
Ile-19	119.36	8.43	4.12	1.42	γH 0.06, 0.94; γH$_3$ −0.22; δH$_3$ 0.66	Ala-73	120.79	7.98	3.79	1.48	
						Thr-74	114.87	7.81	3.96	4.40	γH$_3$ 1.49
Ile-20	130.52	8.82	4.55	1.52	γH$_3$ 0.72	Tyr-75	126.45	8.71	3.48	2.61, 1.81[f]	H(2,6) 5.78, 6.86; H(3,5) 6.38, 2.92
Ala-21	131.21	8.69	2.80	1.21							
Pro-22			4.19	2.36, 2.09	γH 1.88, 1.94; δH 3.37, 3.02	Val-76	109.08	8.03	2.38	(1.03, 0.84)[i]	γH$_3$ 1.71
Asp-23	114.61	7.48	4.44	2.56, 3.03		Lys-77	119.73	6.67	3.95	(1.77)[c]	γH 1.44, δH 1.65, εH 3.08
Gly-24	109.46	8.26	3.33, 4.24								
Thr-25	118.98	7.90	3.76	3.96	γH$_3$ 1.02	Asp-78	106.61	6.32	3.96	2.60, 2.84	
Glu-26	129.92	9.01	4.12	2.35, 1.55	γH 2.07, 1.97	Pro-79			3.43	1.03, 0.35	γH −0.23, 0.69; δH 2.74, 3.07
Ile-27	130.65	7.89	3.84	1.53	γH 0.92, 1.20; γH$_3$ 0.85	Gly-80	105.05	8.34	3.41, 3.78		
						Ala-81	124.79	7.38	3.88	1.27	
Val-28	116.66	8.15	4.04	1.58	γH$_3$ 0.90, 0.93	Phe-82	119.17	7.77	4.16	3.29, 3.44	H(2,6) 7.13, H(3,5) 7.27
Lys-29	131.09	8.80	4.08	1.82, 1.53	γH 1.22, 1.31; δH 1.64; εH 2.93	Leu-83	118.48	7.96	3.69	1.86, 1.08	γH 2.26; δH$_3$ 1.11, 0.90
Gly-30	117.72	7.45	4.25, 3.78								
Ala-31	125.39	6.11	4.54	1.16							
Lys-32	115.40	8.36	4.26	1.52, 2.03[b]	γH 1.18, 1.26; δH 1.56; εH 2.86	Lys-84	117.30	7.93	4.11	1.61, 1.67[b]	
						Glu-85	119.13	7.70	3.99	1.88, 2.00	γH 2.19
Thr-33	117.89	7.29	4.04	4.14	γH$_3$ 1.76	Lys-86	118.71	8.23	3.78	(1.18)[c]	γH 0.53, 0.18; δH (1.14)[c]; εH 2.60, 2.33
Gly-34	104.99	7.10	3.60, −0.65								
Pro-35			3.46	0.97							
Asn-36	119.55	6.73	3.73	2.43, 1.52	γNH$_2$ 8.23, 7.30; γ^{15}N 113.41	Leu-87	116.35	7.91	4.17	1.75, 1.55	γH 1.46; δH$_3$ 0.95, 0.77
Leu-37	125.90	7.95	3.87	0.69, 1.23	γH −0.12; δH$_3$ −1.77, −0.80	Asp-88	121.60	7.50	4.21	2.30, 3.14	
						Asp-89	115.52	7.56	4.81	2.32, 2.51	
Tyr-38	124.22	7.70	3.62	2.66, 2.52	H(2,6) 6.70, H(3,5) 6.79	Lys-90	125.18	8.83	3.90	1.71, 1.91	γH 1.51, εH 2.98[j]
						Lys-91	118.48	8.52	4.31	(1.90)[c]	γH 1.36, δH 1.70, εH 3.01
Gly-39	118.33	7.28	3.78, 3.63								
Val-40	118.06	6.97	3.77	1.63	γH$_3$ 0.91, 0.99	Ala-92	123.97	7.23	3.96	1.23	
Val-41	122.18	8.06	3.51	2.11	γH$_3$ 0.79, 1.01	Lys-93	118.87	8.03[e]	4.79	(1.70)[c]	γH 1.50, 1.37; εH 3.04
Gly-42	119.17	8.92	4.42, 3.65								
Arg-43	125.92	8.38	4.64	2.33, 2.18[d]	γH 1.89	Ser-94	116.65	8.35	4.37	3.58, 0.78	
Thr-44	124.76	8.75	4.32	3.93	γH$_3$ 1.34	Gly-95	87.83	8.62	3.40, 3.57		
Ala-45	135.39	8.67[e]	4.58	1.21		Met-96	126.26	8.58	3.39	−0.04, −2.58	γH −1.51, −3.62; εH$_3$ −2.93
Gly-46	107.40	9.31	3.33, 2.15								
Thr-47	103.71	8.44	4.78	4.56	γH$_3$ 1.11	Ala-97	135.46	8.79	4.10	1.34	
Tyr-48	130.96	8.94[e]	4.65	3.25, 2.99[f]	H(2,6) 7.12, H(3,5) 6.97	Phe-98	120.78	6.45	4.17	0.90, 3.00	H(2,6) 6.96, H(3,5) 7.52
Pro-49			4.27	2.29, 1.76	γH 1.82; δH 2.04, 3.67	Lys-99	121.04	6.14	3.81	1.28, 1.13	γH 0.90, 0.82; δH 1.42, 1.39; εH 2.68, 2.66
Glu-50	115.72	8.64	3.89	(2.30)[c]	γH (2.20)[c]						
Phe-51	122.46	7.71	4.26	2.90, 2.88	H(2−6) 7.13, 7.83	Leu-100	124.51	8.21	4.29	1.61, 1.02	γH,δH$_3$ 1.30, 0.86[k]
Lys-52	129.57	7.23	4.52	1.67, 1.48	γH 1.36, εH 3.04	Ala-101	130.42	8.55	4.04	1.41	
Tyr-53	127.80	8.21	5.16	2.93, 3.90	H(2,6) 8.23, 7.59; H(3,5) 7.59, 7.15; OH 9.95	Lys-102	115.52	7.50	4.65	1.82, 1.73	γH 1.43, εH 3.03[j]
						Gly-103	110.53	8.92	3.94, 4.52		
						Gly-104	112.79	9.13	3.72, 4.00		
Lys-54	122.10	10.18[e]	4.74	2.78, 2.27	γH 1.86	Glu-105	121.42	9.80	4.15	2.16, 2.07[d]	γH 2.51, 2.38
Asp-55	115.43	8.03	4.40	2.76, 2.68		Asp-106	123.73	7.94	4.45	2.90, 2.76	

Table I (Continued)

residues	chemical shifts (ppm)					residues	chemical shifts (ppm)				
	^{15}N	NH	αH	βH	others		^{15}N	NH	αH	βH	others
Val-107	122.46	8.46	4.05	2.39	γH_3 1.65	Ala-112	120.73	7.85	4.07	1.49	
Ala-108	124.71	8.60	4.12	1.73		Ser-113	113.96	7.66	4.31	3.94[l]	
Ala-109	120.24	7.38	4.22	1.47		Val-114	116.43	6.86	3.90	1.93	γH_3 0.44, 0.56
Tyr-110	121.11	8.33	4.36	3.13, 3.58	H(2,6) 6.76, H(3,5) 6.10	Val-115	116.29	6.47	3.92	1.99	γH_3 0.51, 0.58
Leu-111	120.58	8.50	3.44	2.06, 1.01	γH 2.04; δH_3 1.16, 0.50	Lys-116	131.03	7.54	4.19	1.87, 1.76	γH 1.44, δH 1.69, ϵH 3.01

[a] Chemical shifts are in ppm accurate to ±0.01 ppm. ^1H shifts are referenced to dioxane at 3.751 ppm. ^{15}N shifts are referenced to $(^{15}NH_4)_2SO_4$ at 22.3 ppm. Values are for cytochrome c_2 at pH 6 and 30 °C. Atom names are those given in the IUB Recommendations of 1978. [b] There were no NH–βH cross-peaks in R-COSY observed for these spin systems. [c] Cross-peak shape suggests that these methylene protons are degenerate. [d] As only one NH–βH connectivity is observed in R-COSY or DR-COSY, the other βH was based on peak intensity in TOCSY spectra. [e] Determined in ^1H–^{15}N spectra. [f] NH–βH_2 observed in NOESY at 30 °C. αH–βH_2 couplings observed in TOCSY and DQF-COSY experiments. [g] βH at 4.05 ppm in 70-ms TOCSY. [h] Assignment to proton type of the $\gamma H_2\delta H_3$ fragment was by peak intensity in TOCSY experiments. [i] There were no COSY or RELAY peaks to distinguish between the βH and γH_3 resonances. [j] Observed at 40 °C. [k] Two clear NH–βH_2 connectivities in DR-COSY are observed (Figure 6). All observed resonances are tabulated, suggesting that either γH–δH_3 or $(\delta H_3)_2$ is degenerate. [l] βH is at 3.97 ppm in 70-ms TOCSY.

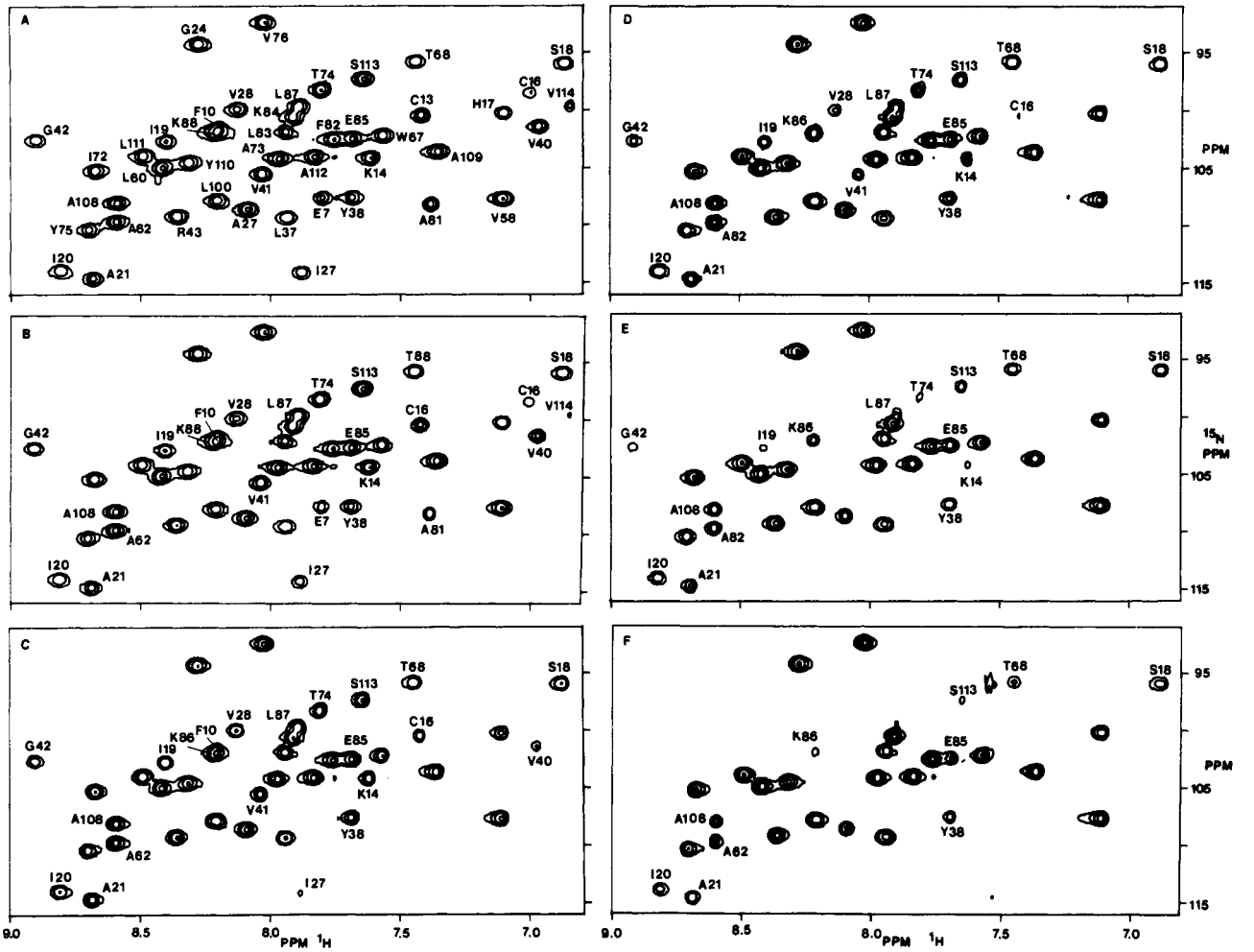

FIGURE 9: Sections of ^1H–^{15}N HMQC spectra of ferrocytochrome c_2 acquired at 30 °C, pH 6, in D_2O. The fully protonated ^{15}N-enriched protein was concentrated, at 4 °C, in a deuterated buffer 80 min before the sample was placed in the spectrometer. Each spectrum was acquired in 30 min. The mid-time point of each spectrum is (A) 50, (B) 80, (C) 265, (D) 685, (E) 1545, and (F) 2460 min. In (A), all correlations are assigned. In subsequent sections, correlations that show an exchange rate within 40 h are assigned.

Figure 9 shows part of 6 of the 10 ^1H–^{15}N HMQC spectra acquired at different time intervals. In these spectra, the resonances of 23 peptide NH protons and the N(1)H of Trp-67 and the folded $N_\pi H$ of His-17 show no change in intensity within 40 h and are therefore considered slowly exchanging under our experimental conditions of 30 °C and pH 6. A further 32 NH protons show appreciable exchange over the 40-h period of the experiment where 29 of these are resolved so that a rate constant can be calculated. The overlapping correlations of Phe-10 and Lys-86 appear to exchange at similar rates; thus, only approximate rate constants can be calculated. The peaks of Phe-82 and Glu-85 are just resolved, but volume integration of the individual peaks is not possible. The peak intensity of Phe-82 shows this proton is slowly exchanging; therefore, a reasonable rate constant can be calculated for the much more rapidly exchanging NH of Glu-85. Figure 10 shows plots of several of these intermediate exchanging resonances which are assigned to NH protons of the N-terminal helix. The sequence locations of the slowly and intermediate exchanging NH protons are shown in Figure 2.

Of the 55 intermediate to slowly exchanging NH protons, 34 are located in helices. Within these helices, as defined by

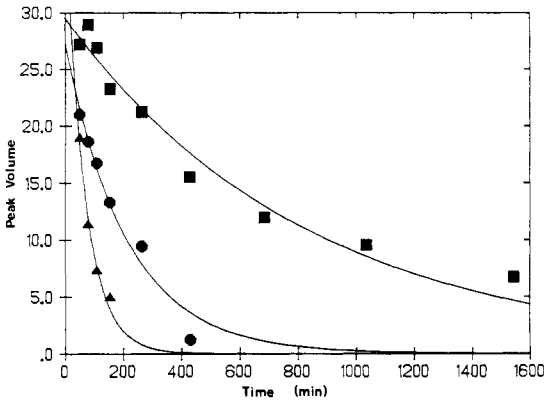

FIGURE 10: Plot of the volume integrals of several exchanging NH protons of the N-terminal helix versus time: (▲) Glu-7; (●) Cys-13; (■) Lys-14. Rate constants (k_m, $min^{-1} \times 10^{-3}$) were calculated by an exponential least-squares analysis: 15 ± 2 (Glu-7), 4.8 ± 0.7 (Cys-13), and 1.2 ± 0.1 (Lys-14).

the short-range NOE data in Figure 2, all NH protons, except the first four of each helix, are expected to form hydrogen bonds that stabilize the helix and therefore show a slowing of exchange. For the long central helix, residues 69–89, 15 NH protons are intermediate to slowly exchanging, with the NH protons of the first 3 and the last residues exchanging rapidly for deuterium. For the short central helix, 55–65, 6 NH protons are slowly and intermediate exchanging, and the first 2 and the last 3 rapidly exchanging. In the C-terminal helix, 103–115, 7 NH protons are slowly and intermediate exchanging, and the first 5 and the last resdiues are rapidly exchanging. For the N-terminal helix, 3–17, the short-range NOE data suggest that this helix is distorted. Within the segment 3–12, two NH protons show intermediate exchange, and the others exchange rapidly. Three NH protons of the final five residues of the N-terminal helix are intermediate exchanging, His-17 is slowly and Thr-15 rapidly exchanging. Of the remaining 21 NH protons, 5 may be involved in stabilizing the neck region of the Ω loop spanning Ile-19 to Val-28 and 1 in the characterized type II turn 40–43. Several of the remainder may be involved in hydrogen bonds with the heme or other groups that remain to be characterized.

Discussion

The combination of ^1H–^1H and ^1H–^{15}N spectroscopy proved valuable in resolving ambiguities due to overlapping resonances and thus determining the near-complete backbone assignments of the *R. capsulatus* ferrocytochrome c_2. The ^1H–^{15}N coupling is large (90 Hz) and almost identical for all peptide ^{15}NH; therefore, correlations are expected for all residues except the amino terminus and Pro. Generally, several correlations may be missing because of saturation transfer (Gronenborn et al., 1989). As the spectra in this study were acquired at pH 6, this problem is sufficiently reduced so that all correlations are observed. However, several resonances do have weak intensities, for example, Lys-32, which is probably a surface residue. The fact that we can observe and almost resolve every ^1H–^{15}N correlation indicates that this spectrum is ideal for investigating backbone fluctuations and stability.

As the NH and αH chemical shifts are determined to a large extent by carbonyl (hydrogen bond) and ring current effects, the structural and sequence homology of the cytochromes would suggest that similar chemical shifts may be expected for analogous residues. However, a comparison of the backbone NH chemical shifts of cytochrome c_2 with those of horse heart cytochrome *c* (Wand et al., 1989) displayed little similarity. While approximately 30% of the analogous residues were less than 0.3 ppm different, an equal number differed by more than 1 ppm. Even a comparison of the helices failed to show a significant similarity, and, therefore, until the tertiary structures of these cytochromes are known, a thorough comparison must wait.

The availability of the ^1H–^{15}N assignments and the ability to acquire 2D spectra in short time periods permitted calculation of exchange rates for intermediate exchanging NH protons and the classification of slowly exchanging NH protons. These data are valuable support for the characterization of the secondary structure of *R. capsulatus* cytochrome c_2 and for obtaining an understanding of its dynamics and stability. For an NH to exchange in a helix, the hydrogen bond must open, requiring a rotation about one of the α-carbon dihedral angles. As the center of the helix is approached, the probability of a hydrogen bond opening is increasingly reduced as the preceding and succeeding hydrogen bonds must be opened (Englander & Kallenbach, 1984). This behavior is observed for 3 of the helices where there are cores of slowly exchanging NH protons: residues 60 and 61 of the short central helix; residues 75–78 and 82–84 of the long central helix which contains a Pro at position 79; residues 109–112 of the C-terminal helix. In each case, this core is flanked with intermediate exchanging protons. There are additional slowly exchanging protons on the N-terminal side of both the short and long central helices whose increased stability must be due to participation in hydrogen bonds, but not for stabilizing the helix.

Surprisingly, the N-terminal helix appears relatively unstable. The peptide NH of His-17 is the only slowly exchanging proton in this helix, while another six protons show rate constants between 0.001 and 0.015 min^{-1}. A recent hydrogen exchange study of horse heart mitochondrial cytochrome *c* showed that the N-terminal α-helix of this protein is markedly stable (Wand et al., 1986). The NH protons of residues 8–15 for this protein showed rate constants of 10^{-4}–0.6 h^{-1} at pH 7 and 20 °C. In the analogous region in cytochrome c_2, only three NH protons showed any slowing of exchange: Glu-7, Phe-10, and Cys-13. These residues are probably on the internal face of the helix, and NH exchange is slowed by not only hydrogen bonding but lack of solvent accessibility. It is noteworthy that these residues are separated by $i + 3$ in each case. On the other hand, in cytochrome *c*, the internal hydrogen-bonded residues of the N-terminal helix, Phe-10 and Cys-14, are $i + 4$ apart, consistent with these residues being on the same face of an α-helix. The short-range NOE data and the NH exchange pattern of the N-terminal helix of *R. capsulatus* cytochrome c_2 suggest that the N-terminal helix of this protein is distorted and not a regular α-helix. The fact that the most slowly exchanging NH protons are $i + 3$ apart suggests tentatively that residues 7–13 are part of a 3_{10} helix. The X-ray crystal structure of *R. rubrum* cytochrome c_2 shows that residues 11–14, equivalent to residues 10–13 in *R. capsulatus*, indeed form a 3_{10} helix (Salemme et al., 1973; Bhatia, 1981).

There are 9 intermediate and slowly exchanging protons in the segment 37–47. Short-range NOE patterns indicate that this region is ordered but nonregular (Figure 2). The analogous region in the X-ray structure of cytochrome c_2 of *R. rubrum* suggest that residues 37–40 and 40–43 should be two type II turns (Salemme et al., 1973; Bhatia, 1981). For the latter turn, NOE data in combination with the slowly exchanging NH of Arg-43 agree that residues 40–43 form a type II turn in *R. capsulatus* cytochrome c_2. NOE data for residues 37–40 do not indicate the presence of a turn here, although

the NH of Val-40, which would stabilize this turn, exchanges with a rate constant of 0.006 min^{-1}, suggesting that it participates in a hydrogen bond. The NOE data indicate that there may be another type II turn between residues 35 and 38 (Figure 2). Unexpectedly, the NH of Leu-37 is slowly exchanging, compared to the NH of Tyr-38 (0.003 min^{-1}) whose NH proton would be stabilizing this turn. Significantly, the X-ray data for *R. rubrum* cytochrome c_2 do not show a turn in this region. This segment on the right side of the heme is highly conserved in the cytochromes with the carbonyl of Pro-35 participating in a hydrogen bond with the $N_\pi H$ of His-17.

In the X-ray structure of *R. rubrum* cytochrome c_2, there are an additional three reverse turns. In the analogous regions of *R. capsulatus* cytochrome c_2, 20–23, 48–51, and 89–92, the NOE data show a reverse turn only for the latter segment. It is noted that the NH proton stabilizing this reverse turn exchanges faster than these experiments can detect (>0.05 min^{-1}). For the former two regions, in *R. capsulatus* cytochrome c_2, there are Pro substitutions which may provide a sufficient turn in the polypeptide chain. Furthermore, in this protein, there is a 6-residue insertion succeeding segment 20–23. The NOE data (Figure 2) show that the region encompassing 19–28 forms an Ω loop which provides a reversal in the polypeptide chain.

It is interesting that for the four possible reverse turns, the NH protons that are supposed to participate in the hydrogen bonds that stabilize these turns are relatively rapidly exchanging. It is most unlikely that simply increased solvent accessibility is responsible for these apparent instabilities. The NH protons of the hydrogen bonds of these turns are relatively isolated from other slowly or intermediate exchanging NH protons. Thus, hydrogen-bond breakage is less dependent on the simultaneous breakage of neighboring bonds compared to the helices. For Ala-92, the residue that would stabilize the turn 89–92, there are no slowly exchanging NH protons within 5 residues. Therefore, the exchange of this hydrogen bond is not synergistic, and consequently, NH exchange is relatively fast.

This preliminary investigation of the NH exchange of ferrocytochrome c_2 indicates the relative ease of determining NH exchange rate constants from 2D ^1H–^{15}N data. Previous workers have suggested that ^1H–^{15}N HMQC spectra can be acquired on enriched proteins in time periods of less than 2 h (McIntosh et al., 1987). In this study, it has been shown that the experiment can be acquired in even shorter time periods of 10–30 min for samples of 2–3 mM protein, thus permitting a reasonably accurate rate constant to be calculated for all protons with half-lives longer than approximately 60 min. This application can easily be used to compare the stability of various mutants and thus address questions of the importance of specific hydrogen bonds for the structural stability of a protein or the functional significance of these bonds. For example, this method has been applied to a comparison of the intermediate exchanging NH protons of wild *R. capsulatus* cytochrome c_2 and a mutant cytochrome c_2 in which the highly conserved Pro-35 is substituted with Ala. Preliminary NH exchange data show that the exchange rate of the NH of Gly-34 changes from a rate of 0.005 min^{-1} in the wild protein to a rate faster than can be detected by these experiments (>0.05 min^{-1}) in the mutant protein. This work will be the subject of a later publication.

Added in Proof

Ser-94 should be Thr-94. Resonances assigned to Gly-95 should be assigned to the ϵNH–δNH_2 resonances of Arg-43. The resonances of Gly-95 are 8.38, 3.71/4.63 ppm (NH–αH_2).

Registry No. Ferrocytochrome c_2, 9035-43-2.

References

Baccarini-Melandri, A., Jones, O. T. G., & Hauska, G. (1978) *FEBS Lett. 86*, 151–154.

Bartsch, R. G. (1978) *The Photosynthetic Bacteria* (Clayton, R. K., & Sistron, W. R., Eds.) p 253, Plenum, New York.

Bax, A., & Marion, D. (1988) *J. Magn. Reson. 78*, 186–191.

Bax, A., Griffey, R. H., & Hawkins, B. L. (1983) *J. Magn. Reson. 55*, 301–315.

Bhatia, G. E. (1981) Ph.D. Thesis, University of California, San Diego.

Braunschweiler, L., & Ernst, R. R. (1983) *J. Magn. Reson. 53*, 521–528.

Cusanovich, M. A., Meyer, T. E., & Tollin, G. (1988) *Advances in Inorganic Biochemistry, Heme Proteins 7* (Eichhorn, G. L., & Manzilli, L. G., Eds.) pp 37–92, Elsevier, New York.

Daldal, F., Cheng, S., Applebaum, J., Davidson, E., & Prince, R. (1986) *Proc. Natl. Acad. Sci. U.S.A. 83*, 2012–2016.

Davis, D. G., & Bax, A. (1985) *J. Am. Chem. Soc. 107*, 2820–2821.

Englander, S. W., & Kallenbach, N. (1984) *Q. Rev. Biophys. 16*, 521–655.

Englander, S. W., & Wand, A. J. (1987) *Biochemistry 26*, 5953–5958.

Ernst, R. R. (1988) *XIII International Conference on Magnetic Resonance in Biological Systems*, Madison, WI.

Folkers, P. J. M., Clore, G. M., Driscoll, P. C., Dodt, J., Kohler, S., & Gronenborn, A. M. (1989) *Biochemistry 28*, 2601–2617.

Gronenborn, A. M., Bax, A., Wingfield, P. T., & Clore, G. M. (1989) *FEBS Lett. 243*, 93–98.

Holden, H. M., Meyer, T. E., Cusanovich, M. A., Daldal, F., & Rayment, I. (1987) *J. Mol. Biol. 195*, 229–231.

International Union of Biochemistry (1978) *Biochemical Nomenclature & Related Documents*, Clowes & Son, London.

Jeener, J., Meier, B. H., Bachmann, P., & Ernst, R. R. (1979) *J. Chem. Phys. 71*, 4546–4553.

Leszczynski, J. F., & Rose, G. D. (1986) *Science 234*, 849–855.

McIntosh, L. P., Griffey, R. H., Muchmore, D. C., Nielson, C. P., Redfield, A. G., & Dahlquist, F. W. (1987) *Proc. Natl. Acad. Sci. U.S.A. 84*, 1244–1248.

Meyer, T. E., & Kamen, M. D. (1982) *Adv. Protein Chem. 35*, 105–212.

Miki, K., Saeda, M., Masaki, K., Kasai, N., Miki, M., & Hayashi, K. (1986) *J. Mol. Biol. 191*, 579–580.

Otting, G., Widmer, H., Wagner, G., & Wüthrich, K. (1986) *J. Magn. Reson. 66*, 187–193.

Pielak, G. J., Atkinson, R. A., Boyd, J., & Williams, R. J. P. (1988a) *Eur. J. Biochem. 177*, 179–185.

Pielak, G. J., Boyd, J., Moore, G. R., & Williams, R. J. P. (1988b) *Eur. J. Biochem. 177*, 167–177.

Rance, M. (1987) *J. Magn. Reson. 74*, 557–564.

Rance, M., Sørensen, O. W., Bodenhausen, G., Wagner, G., Ernst, R. R., & Wüthrich, K. (1983) *Biochem. Biophys. Res. Commun. 117*, 479–485.

Redfield, A. G., & Kuntz, S. D. (1975) *J. Magn. Reson. 19*, 250–254.

Redfield, C., & Dobson, C. M. (1988) *Biochemistry 27*, 122–136.

Rickle, G. K., & Cusanovich, M. A. (1979) *Arch. Biochem. Biophys. 197*, 589–598.

Salemme, F. R., Kraut, J., & Kamen, M. D. (1973) *J. Biol. Chem. 248*, 7701-7716.
Senn, H., & Wüthrich, K. (1983) *Biochim. Biophys. Acta 746*, 48-60.
Stockman, B. J., Reily, M. D., Westler, W. M., Ulrich, E. L., & Markley, J. L. (1989) *Biochemistry 28*, 230-236.
Tollin, G., Meyer, T. E., & Cusanovich, M. A. (1986) *Biochim. Biophys. Acta 853*, 29-41.
Torchia, D. A., Sparks, S. W., & Bax, A. (1988) *Biochemistry 27*, 5135-5141.
Wagner, G. (1985) *J. Magn. Reson. 55*, 151-156.
Wagner, G., Neuhaus, D., Wörgötter, E., Vaŝák, M., Kägi, J. R. H., & Wüthrich, K. (1986) *J. Mol. Biol. 187*, 131-135.
Wand, A. J., Roder, H., & Englander, S. W. (1986) *Biochemistry 25*, 1107-1114.
Wand, A. J., Di Stefano, D. L., Feng, Y., Roder, H., & Englander, S. W. (1989) *Biochemistry 28*, 186-194.
Weaver, P. F., Wall, J. D., & Gest, H. (1975) *Arch. Microbiol. 105*, 207-216.
Wüthrich, K. (1986) *NMR of Proteins and Nucleic Acids*, Wiley, New York.
Yu, L., & Smith, G. (1988) *Biochemistry 27*, 1949-1956.

N-Methyl-D-aspartate/Phencyclidine Receptor Complex of Rat Forebrain: Purification and Biochemical Characterization†

Annat F. Ikin, Yoel Kloog, and Mordechai Sokolovsky*

Laboratory of Neurobiochemistry, Department of Biochemistry, The George S. Wise Faculty of Life Sciences, Tel Aviv University, Tel Aviv 6997, Israel

Received July 31, 1989; Revised Manuscript Received October 20, 1989

ABSTRACT: The *N*-methyl-D-aspartate (NMDA)/phencyclidine (PCP) receptor from rat forebrain was solubilized with sodium cholate and purified by affinity chromatography on amino-PCP–agarose. A 3700-fold purification was achieved. Polyacrylamide gel electrophoresis in the presence of sodium dodecyl sulfate and dithiothreitol revealed four major bands of M_r 67 000, 57 000, 46 000, and 33 000. [^{3}H]Azido-PCP was irreversibly incorporated into each of these bands after UV irradiation. The dissociation constant (K_d) of [1-(2-thienyl)cyclohexyl]piperidine ([^{3}H]TCP) binding to the purified NMDA/PCP receptor was 120 nM. The maximum specific binding (B_{max}) for [^{3}H]TCP binding was 3.3 nmol/mg of protein. The pharmacological profile of the purified receptor complex was similar to that of the membranal and soluble receptors. The binding of [^{3}H]TCP to the purified receptor was modulated by the NMDA receptor ligands glutamate, glycine, and NMDA.

The *N*-methyl-D-aspartate (NMDA)[1] type of excitatory amino acid receptor is one of the best characterized glutamate receptors in the mammalian central nervous system. These receptors, which are ligand-gated cation channels, are involved in synaptic plasticity (Artola & Singer, 1987; Collingridge, 1987) and in long-lasting enhancement of synaptic efficacy (i.e., long-term potentiation), thought to be the basis of processes involved in learning and memory (Collingridge et al., 1983; Collingridge & Bliss, 1987). Overactivation of these receptors is associated with epileptogenic seizures (Turski et al., 1985), neurotoxicity (Rottman & Olney, 1987), and neuronal loss due to hypoglycemia (Rottman & Olney, 1987) and ischemia (Cotman & Iversen, 1987; Kemp et al., 1987).

The role of dissociative anesthetics, such as PCP and related drugs, as open-channel blockers of NMDA receptors (Honey et al., 1985; Foster & Wong, 1987; Kloog et al., 1988), as well as the notion of a high-affinity NMDA/PCP receptor complex, is well established. Therefore, in recent years PCP and its analogues have been used as biochemical probes of NMDA receptor channel activation.

We recently described the successful solubilization of high-affinity PCP-binding sites from rat forebrain membranes, utilizing the anionic detergent sodium cholate (Ambar et al., 1988). The binding of [^{3}H]TCP, a potent PCP analogue, was shown to be modulated by NMDA receptor ligands, thus providing further evidence for the existence of an NMDA/PCP receptor complex. We now describe the purification of the solubilized NMDA/PCP receptor complex by affinity chromatography.

Experimental Procedures

Materials. [^{3}H]TCP (28.6 Ci/mmol) and [^{3}H]AZ-PCP (16.8 Ci/mmol) were purchased from Israel Nuclear Center (Negev, Israel). Dexoxadrol and levoxadrol were donated by Dr. A. E. Jacobsen (National Institutes of Health). MK-801 was a gift from Merck Sharp & Dohme Research Laboratories. PCP and NH_2-PCP were a gift from Dr. A. Kalir (Tel-Aviv University). The synthesis of NH_2-PCP has been described by Kalir et al. (1978). NMDA and DL- and D-AP-5

†This work was supported in part by the National Institutes of Health, Grant 5RO1 DA04168-03, and The Julius Bär Foundation (Zurich).
*To whom correspondence should be addressed.

[1] Abbreviations: NMDA, *N*-methyl-D-aspartate, PCP, phencyclidine; SDS–PAGE, sodium dodecyl sulfate–polyacrylamide gel electrophoresis; EDTA, ethylenediaminetetraacetic acid; EGTA, ethylene glycol bis(β-aminoethyl ether)-*N*,*NN*′,*N*′-tetraacetic acid; AP-5, D-(−)-2-amino-5-phosphovalerate; AZ-PCP, *N*-[1-(3-azidophenyl)cyclohexyl]piperidine; PMSF, phenylmethanesulfonyl fluoride; TCP, [1-(2-thienyl)cyclohexyl]piperidine; Glu, glutamate; Gly, glycine; EC_{50}, concentration causing 50% of maximal effect; DTT, dithiothreitol.

0006-2960/90/0429-2290$02.50/0